

Article

Enhanced Electrochromic Properties of Nanostructured WO₃ Film by Combination of Chemical and Physical Methods

Xiaoni Li ¹, Zhijie Li ¹, Wanting He ¹, Haolin Chen ¹, Xiufeng Tang ^{1,2,*}, Yeqing Chen ^{1,*} and Yu Chen ^{3,*}

¹ School of Applied Physics and Materials, Wuyi University, Jiangmen 529020, China; nx10909168@163.com (X.L.); z598414677@outlook.com (Z.L.); oneselfhappy@foxmail.com (W.H.); 13226254599@163.com (H.C.)

² Research Center of Flexible Sensing Materials and Devices, Wuyi University, Jiangmen 529020, China

³ Analysis and Test Center, Guangdong University of Technology, Guangzhou 511400, China

* Correspondence: xiufengtang@wyu.edu.cn (X.T.); yeqingchen@ciac.ac.cn (Y.C.); atc_chenyu@gdut.edu.cn (Y.C.)

Abstract: WO₃ films are the most widely used electrochromic functional layers. It is known that WO₃ films prepared by pure chemical method generally possess novel nanostructures, but the adhesion between WO₃ films and substrates is weak. However, WO₃ films prepared by pure physical method usually show relatively dense morphology, which limits their electrochromic properties. In order to break through these bottlenecks and further improve their electrochromic properties, this work first prepared nanostructured WO₃ powder by chemical method, and then using this powder as the evaporation source, nanostructured WO₃ films were fabricated by vacuum thermal evaporation method. Properties of nanostructured WO₃ films were systematically compared with those of ordinary WO₃ films. It turned out that the nanostructured WO₃ film exhibited better cyclic stability and memory effect, and also the optical modulation rate was 14% higher than that of the ordinary WO₃ film. More importantly, the nanostructured WO₃ film showed better adhesion with the ITO substrates. These results demonstrate that a combination of chemical and physical methods is an effective preparation method to improve the electrochromic properties of WO₃ films.

Keywords: WO₃ film; nanostructured; electrochromic; combination of chemical and physical methods



Citation: Li, X.; Li, Z.; He, W.; Chen, H.; Tang, X.; Chen, Y.; Chen, Y. Enhanced Electrochromic Properties of Nanostructured WO₃ Film by Combination of Chemical and Physical Methods. *Coatings* **2021**, *11*, 959. <https://doi.org/10.3390/coatings11080959>

Academic Editor: Emmanuel Koudoumas

Received: 7 June 2021

Accepted: 7 August 2021

Published: 12 August 2021

Publisher's Note: MDPI stays neutral with regard to jurisdictional claims in published maps and institutional affiliations.



Copyright: © 2021 by the authors. Licensee MDPI, Basel, Switzerland. This article is an open access article distributed under the terms and conditions of the Creative Commons Attribution (CC BY) license (<https://creativecommons.org/licenses/by/4.0/>).

1. Introduction

Tungsten oxide (WO₃) has been regarded as the most promising electrochromic material due to its wide range of continuously adjustable optical properties, excellent reversibility, low energy consumption, high coloration efficiency, and environmental friendliness [1–3]. WO₃ films have been used in electrochromic smart windows [4,5], information display [6], photocatalysis [7,8], and energy storage technologies [9,10]. Therefore, further improving the properties of WO₃ films has become one of the research hot spots.

As we know, the electrochemical properties of WO₃ films depend strongly on their preparation method, morphology and structure. Owing to the high surface activity and loose morphology, nanostructured WO₃ can accelerate the electrochemical process and improve the electrochromic properties with respect to the bulk counterparts [11–14]. So far, various nanostructured WO₃, such as nanowires [15], nanorods [16,17], nanocolumnar films [18] and nanoparticles [19] have been prepared and shown good electrochromic properties. Nanostructured WO₃ films have been fabricated by various physical and chemical methods, including sol-gel [20], hydrothermal [21], magnetron sputtering [22] and electron-beam evaporation [23], which are just pure chemical or physical methods. Though WO₃ films prepared by pure chemical method generally possess novel nanostructures, the adhesion between WO₃ films and substrates is weak. On the other hand, WO₃ films prepared by pure physical method such as vacuum thermal evaporation and magnetron sputtering have many advantages, but their morphology is relatively dense, which limits

the electrochromic properties [24]. Therefore, WO_3 films prepared by pure chemical or physical methods lead to the property bottleneck to some extent [25].

Herein, instead of using pure chemical method or pure physical method, nanostructured WO_3 films were prepared by combination of chemical and physical methods. First, nanostructured WO_3 powder was prepared through chemical synthesis, and then nanostructured WO_3 films were fabricated using vacuum thermal evaporation. Their characterization and electrochromic properties were compared with ordinary WO_3 films at the same thickness. Particularly, herein the adhesion between the WO_3 film and the substrate was discussed, which was a key factor in real application of the electrochromic devices but was rarely present in the literature.

2. Materials and Methods

2.1. Sample Preparation

The preparation process was shown in Figure 1. The same amount of 0.025 mol $\text{Na}_2\text{WO}_4 \cdot 2\text{H}_2\text{O}$ and CaCl_2 were respectively dissolved in 50 mL of deionized water, and 0.5 mol/L Na_2WO_4 solution and CaCl_2 solution were prepared. Then, the two solutions were mixed together and HCl was added to adjust the solution pH to be neutral and left to stand for 72 h. The precipitate was filtered and dried at 70 °C to obtain CaWO_4 powder. Next, CaWO_4 powder was dissolved in 100 mL 20% HCl. After standing for 24 h, nanostructured WO_3 powder was obtained by filtration and drying. In the end, the powder was annealed at 500 °C for 2 h.

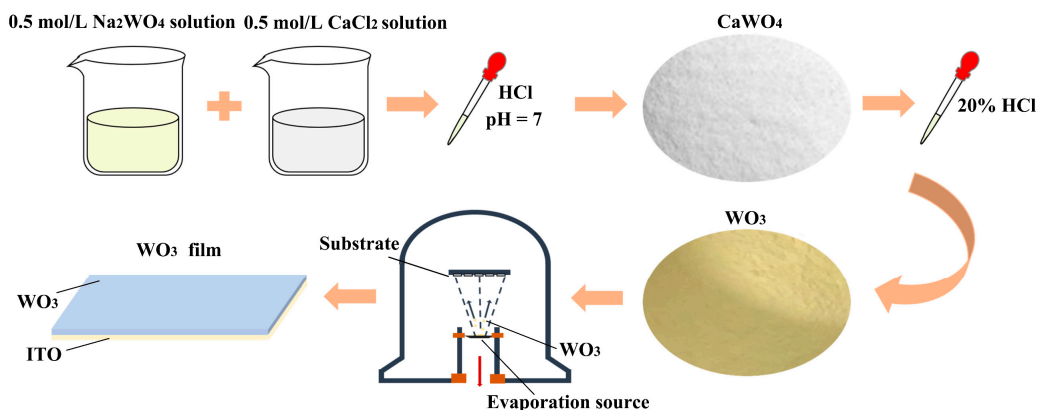


Figure 1. Preparation process diagram of nanostructured WO_3 powder and film.

The indium tin oxide (ITO) glass substrate was used and first subjected to cleaning of acetone, alcohol and deionized water. Then, the nanostructured WO_3 film was prepared by vacuum thermal evaporation (ZHD-300N, Technol, Beijing, China) using the nanostructured WO_3 powder as the evaporation source. The distance between substrates and the evaporation source was 11.5 cm. Oxygen and argon were let into the vacuum chamber with the flow ratio of 2:3, where oxygen was introduced to avoid the WO_3 vapor from being depleted of oxygen during the long-time evaporation [26], ensuring the WO_3 deposition on the substrate. The working pressure was 1.0 Pa, and the temperature of the tungsten boat was kept at 1100 °C for 1.5 h. At this time, the temperature of the substrate varied slightly in the range of 340–350 °C. The substrate rotated at the speed of 10 r/min during the whole process. Finally, nanostructured WO_3 films were obtained at a thickness of about 400 nm. In addition, ordinary WO_3 films with the same thickness were prepared by extending the evaporation time to 2 h for comparing their electrochromic properties, but the other evaporation parameters were kept the same, but using ordinary WO_3 powder as an evaporation source. The deposition rate of the nanostructured WO_3 film was faster originating from its large specific surface area. It should be noted that different deposition rates would inevitably cause different microstructures of the deposited film. However, for comparing their electrochromic properties, the thickness of the two WO_3 films should be

the same, because the optical modulation rate, the memory effect, the adhesion and the cyclic stability all greatly depend on the thickness of the electrochromic film.

2.2. Characterization

Morphology of two kinds of WO_3 powder and two kinds of WO_3 films was observed by scanning electron microscopy (SEM) using a Sigma 500 instrument (Zeiss, Oberkochen, Germany). The structure was examined by X-ray diffraction (XRD) analysis using a Cu K α radiation (Philips X'Pert diffractometer, Amsterdam, The Netherlands). X-ray photoelectron spectroscopy (XPS) analysis was performed by using a Thermo Fisher Scientific ESCALAB 250 XPS system, Waltham, MA, USA. The cyclic stability of WO_3 film was measured by cyclic voltammetry (CV) and the response time was tested by electrochemical double potential step chronograph current test (CA) on an electrochemical workstation (CHI760E). A three-electrode system was formed using WO_3 film as the working electrode, Ag/AgCl as the reference electrode, metal Pt plate as the counter electrode, and 1 mol/L LiClO_4 -PC solution as the electrolyte. CV test was carried out with the voltage ranging from -0.8 V to $+0.8$ V at a scan rate of 100 mV/s. The CA test was conducted at -0.8 V (coloring) and $+0.8$ V (bleaching) for 20 s. Optical transmittance spectra of WO_3 films at colored state and bleached state were examined at wavelength ranging from 200 to 800 nm using an ultraviolet/visible (UV/VIS) spectrophotometer (Shimadzu UV-2550, Tokyo, Japan). The adhesion between WO_3 films and ITO substrates was examined by using ScotchTM adhesive tape (3M, St. Paul, MN, USA) with the adhesion force of 4.7 N/cm.

3. Results and Discussion

3.1. Morphology and Structure

The morphology of both the nanostructured WO_3 powder prepared by the chemical method and the ordinary commercially-bought WO_3 powder was analyzed in detail by SEM as shown in Figure 2. The as-prepared nanostructured WO_3 powder before annealing showed the shape of nanosheets (Figure 2ai). Its size and distribution were uniform. The WO_3 nanosheets were cross-aggregated to form clusters. After annealing at 500 °C, the WO_3 powder still showed uniformly nanoclusters (Figure 2a_{ii}). For comparison, the ordinary WO_3 powder showed a disordered state, among which some clusters were huge and some were tiny (Figure 2b). XRD was employed to analyze the crystal structure and phase properties of the two above WO_3 powder. As can be seen in Figure 3a, both the nanostructured WO_3 powder (Figure 3ai) and ordinary WO_3 powder (Figure 3a_{ii}) were monoclinic and had the three main diffraction peaks at 23.1°, 23.6° and 24.4°, suggesting that these two kinds of WO_3 powder had the same crystalline structure. However, the nanostructured WO_3 powders showed a bulging peak at 15–23°, suggesting that an amorphous component existed, which demonstrated that the coexistence of crystalline phase and amorphous phase was obtained. Furthermore, the high resolution XPS pattern of element W both in the nanostructured WO_3 powder after annealing and ordinary WO_3 powder were depicted in Figure 3b, which were the same. The peak energies of 35.3 and 37.5 eV were attributed to $\text{W}4f_{7/2}$ and $\text{W}4f_{5/2}$, respectively, which corresponded to tungsten atoms in a W^{6+} formal oxidation state.

Two kinds of WO_3 films were prepared by vacuum thermal evaporation respectively using the annealed nanostructured powder and the ordinary powder. It can be seen that the nanostructured WO_3 film was composed of uniform nano-sheets, and there was no crack on the surface, as shown in Figure 4a. While the ordinary WO_3 film was composed of loose agglomerated clusters, the surface cracked seriously, as illustrated in Figure 4b. Besides the evaporation source, deposition conditions would also be responsible for the different microstructures of the two WO_3 films, which were tried to keep the same except the evaporation time. Faster deposition rate of the nanostructured WO_3 film originating from its large specific surface area would cause different grain sizes and different morphologies. As can be seen in Figure 5a, XRD spectra of the two WO_3 films on the ITO glass substrates showed that except for the diffraction peaks corresponding to the ITO substrate, there were

no other obvious diffraction peaks. Both of them were amorphous, mainly because the substrate temperature was not high enough during the evaporation process. As depicted in Figure 5b, only W^{6+} spin-orbit doublets existed in the XPS spectra of the W4f core level, proving the two films were both WO_3 .

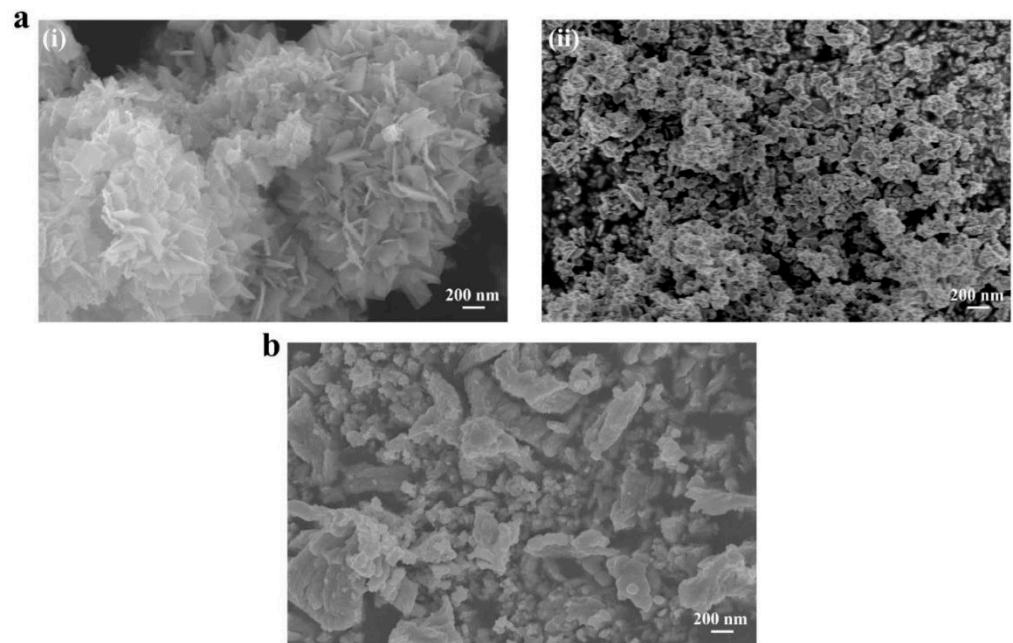


Figure 2. SEM images of the WO_3 powder. (a) nanostructured WO_3 powder before annealing, (a)ii) nanostructured WO_3 powder after annealing. (b) ordinary WO_3 powder.

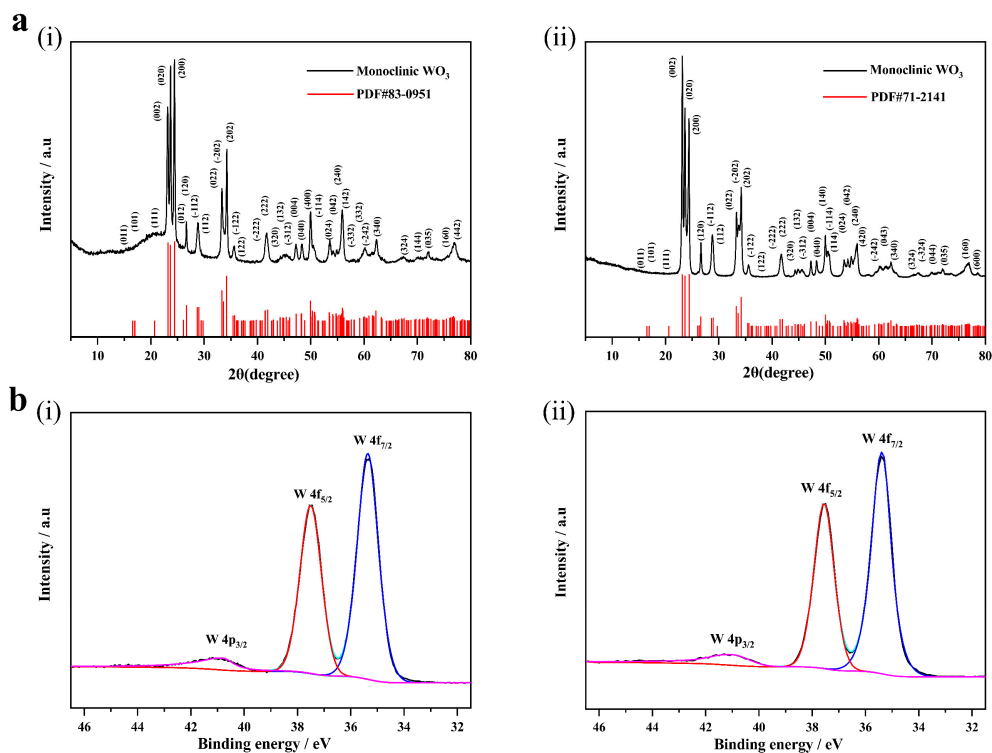


Figure 3. XRD and XPS spectra of the WO_3 powder. (a) XRD spectrum of nanostructured WO_3 powder after annealing, (a)ii) XRD spectrum of ordinary WO_3 powder, (b) XPS spectrum of nanostructured WO_3 powder after annealing, (b)ii) XPS spectrum of ordinary WO_3 powder.

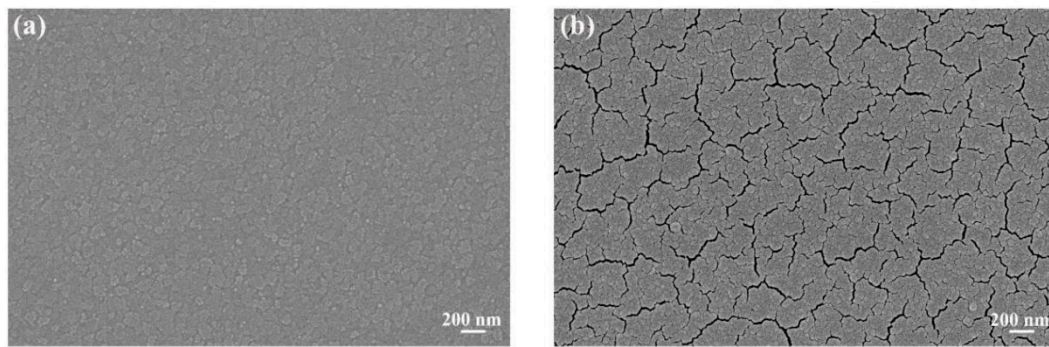


Figure 4. SEM images of the WO₃ films. (a) nanostructured WO₃ film, (b) ordinary WO₃ film.

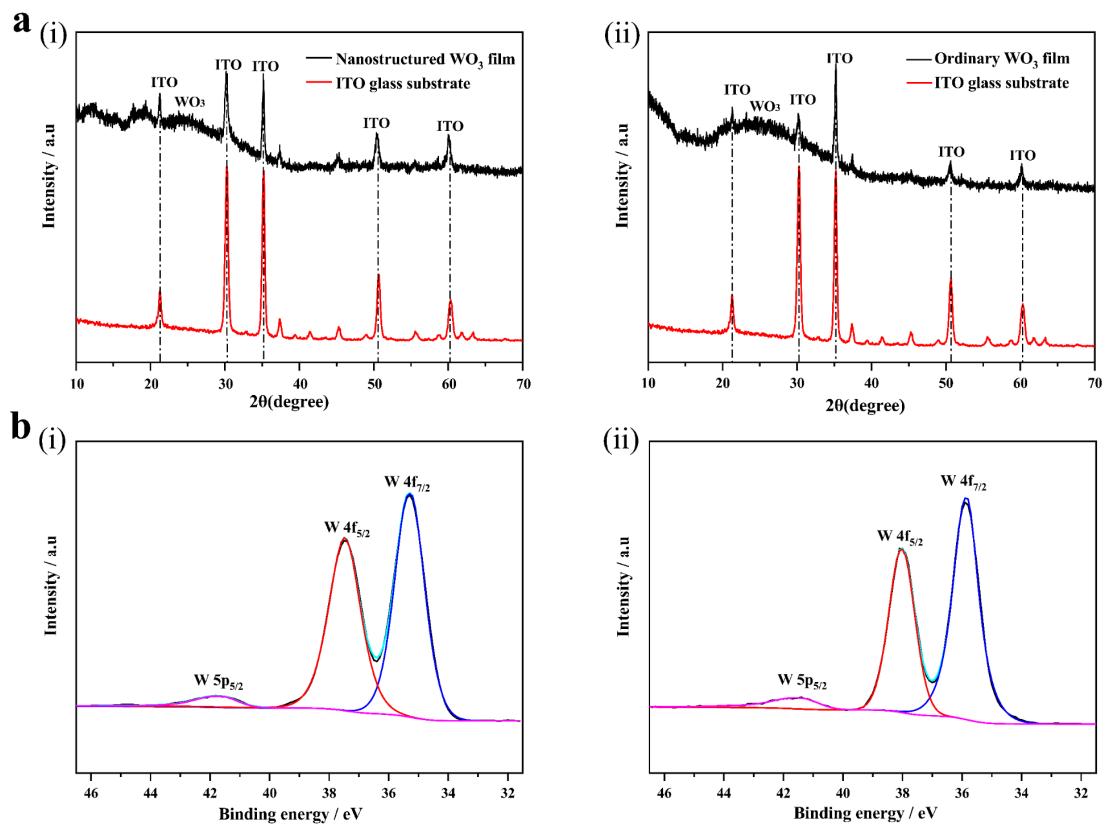


Figure 5. XRD and XPS spectra of nanostructured WO₃ film and ordinary WO₃ film. (ai) XRD spectrum of nanostructured WO₃ film, (aii) XRD spectra of ordinary WO₃ film, (bi) XPS spectrum of nanostructured WO₃ film, (bii) XPS spectrum of ordinary WO₃ film.

3.2. Electrochromic Properties

Response time of the WO₃ film was recorded by the current-time curve, as shown in Figure 6. The response time was usually taken as 90% of the current change value. The coloring time (t_1) and the bleaching time (t_2) of the nanostructured WO₃ film were 8.40 and 1.39 s, respectively, while those of the ordinary WO₃ film were 9.27 and 3.82 s, respectively.

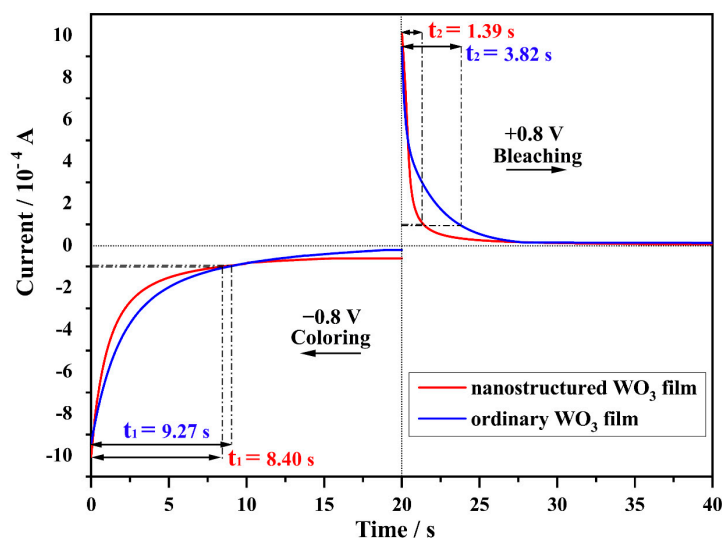


Figure 6. Response time of nanostructured WO_3 film and ordinary WO_3 film.

CV tests were carried out to record Li^+ insertion/ extraction processes of the two WO_3 films, as shown in Figure 7a. The results showed that the area enclosed by the CV curve of the ordinary WO_3 film shrunk rapidly during long-term cycling (Figure 7a(ii)). After 1000 cycles, the ion capacity of the ordinary WO_3 film decreased rapidly from 5.69 to 1.08 $\text{mC}\cdot\text{cm}^{-2}$ and the decreasing rate was as high as 81%, indicating that its cycling stability was poor. However, the CV curve of the nanostructured WO_3 film changed less (Figure 7a(i)), and the ion capacity decreased from 6.08 to 2.81 $\text{mC}\cdot\text{cm}^{-2}$ after 1000 cycles, which was 53% lower than that of the first cycle. Therefore, the nanostructured WO_3 film showed better cycling stability than the ordinary WO_3 film. The optical modulation rates at wavelength of 550 and 633 nm ($\Delta T_{550\text{nm}}$ and $\Delta T_{633\text{nm}}$) were obtained by comparing the transmittances of the two WO_3 films in a fully colored state and a fully-bleached state. The results were represented in Figure 7b. The film was colored or bleached at the potential of 3 V for 2 min. The optical modulation rates of the nanostructured WO_3 film were 43.44% at 550 nm and 55.92% at 633 nm (Figure 7b(i)). However, the optical modulation rates of the ordinary WO_3 film were only 28.64% at 550 nm and 40.68% at 633 nm (Figure 7b(ii)). It was known that the $\Delta T_{550\text{nm}}$ and $\Delta T_{633\text{nm}}$ of the nanostructured WO_3 film were 14% higher than that of the ordinary WO_3 film. As to the memory effect, transmittance of the nanostructured WO_3 film at 633 nm increased by 21.14% after being fully-colored for 8 h (Figure 7c(i)), while that of the ordinary WO_3 film increased by 33.68% (Figure 7c(ii)), which was close to the transmittance of the bleached state. Hence, the nanostructured WO_3 film showed a better memory effect.

The adhesion between the two WO_3 films and the ITO glass substrate was tested by adhesive tape method and the testing process could be divided into three steps. First, the transmittance of the WO_3 film at 550 nm in initial state (T_0) was measured by UV/VIS spectrophotometer. Second, the ScotchTM adhesive tape at the force of 4.7 N/cm was leveled and tightly attached to the surface of the WO_3 film. Then the tape was torn up and the transmittance of the WO_3 film at 550 nm was measured again (T_n). Finally, the adhesion factor f was calculated according to the equation $f = 1 - (T_n - T_0)/(100 - T_0)$. The closer the value of f was to 1, the greater the adhesion of the WO_3 film was. Because at this time almost no film was attached to the adhesive tape. On the contrary, the closer the value of f got to 0, the worse the adhesion of the WO_3 film was. At this moment, the whole film was almost adhered to the adhesive tape. The calculated adhesion factor f was shown in Figure 8. It was observed that the adhesion factor f of the nanostructured WO_3 film was 0.99702, while that of the ordinary WO_3 film was only 0.57148. Consequently, the nanostructured WO_3 film with greater adhesion was more reliable in practical applications,

which provided a potential solution for the adhesion problem in chemical fabrication of films.

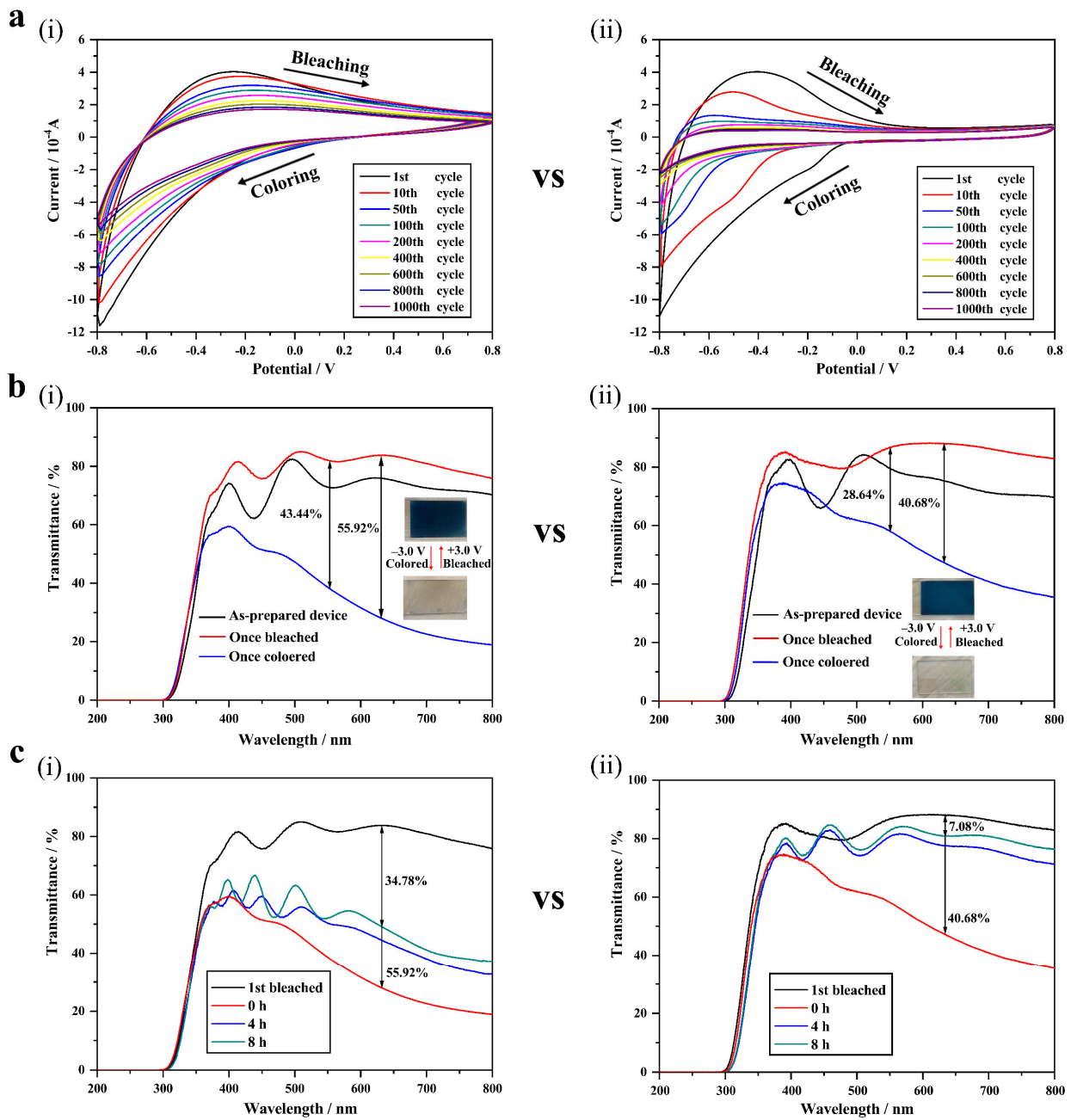


Figure 7. Comparison of the electrochromic properties of the nanostructured WO_3 film (i) and the ordinary WO_3 film (ii). (a) the cyclic stability, (b) the optical modulation rates, (c) the memory effect.

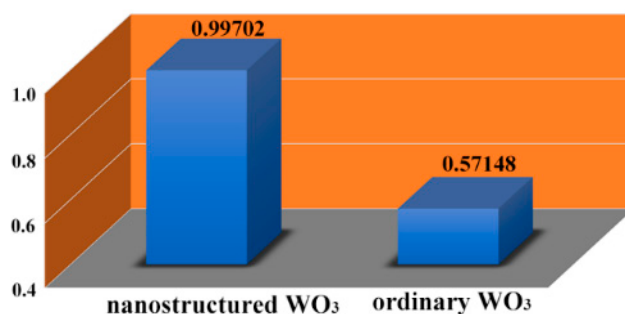


Figure 8. Adhesion of the nanostructured WO₃ film and the ordinary WO₃ film.

Electrochromic properties of the two WO₃ films were summarized in Table 1. Faster response time of the nanostructured WO₃ film originated from its nano-blade morphology (seen in Figure 4a), which reduced the accumulation and accelerated the ion diffusion rate of Li⁺ [27]. The surface of the nanostructured WO₃ film was smooth and uniform, which was conducive to improving the cycling stability. What is more, the nanostructured WO₃ film had excellent adhesion with the ITO substrate because of its uniform and continuous structure, while poor adhesion of the ordinary WO₃ film probably originated from the cracking morphology (Figure 4b). These results indicate that a combination of chemical and physical methods is effective in improving the properties of electrochromic films. The above findings were verified several times and they showed good reproducibility. However, it should be mentioned that the electrochromic properties of the prepared nanostructured WO₃ films were not outstanding when compared with those recently reported, such as the optical modulation of the nanocolumnar structured WO₃ film reaching 65% at the wavelength of 600 nm [18]. In Quy's work, the response times of the PVE-WO₃ film reached 2.9 and 2.1 s, respectively, for the coloring and bleaching process [19].

Table 1. Comparison between the nanostructured WO₃ film and the ordinary WO₃ film.

Electrochromic Properties	Nanostructured WO ₃ Film	Ordinary WO ₃ Film
response time (coloring time/bleaching time)	8.40 s/1.39 s	9.27 s/3.82 s
cycling stability (ion capacity decreasing rate)	53%	81%
optical modulation rates ($\Delta T_{550\text{nm}}$ and $\Delta T_{633\text{nm}}$)	43.44%/55.92%	28.64%/40.68%
memory effect (transmittance increasing rate)	21.14%	33.68%
adhesion (value of adhesion factor)	0.99702	0.57148

4. Conclusions

In this study, nanostructured WO₃ films were prepared by the two-step method. First nanostructured WO₃ powder was chemically synthesized, and then nanostructured WO₃ films were prepared by vacuum evaporation using the nanostructured powder as the evaporation source. With continuous and uniform nano-blade morphology, the nanostructured WO₃ film showed better electrochromic properties than that of the ordinary WO₃ film with better cycling stability and memory effect, stronger adhesion to the ITO substrate, a 14% higher modulation rate and a faster response time. Our research provides an idea for preparing films with better properties by combination of different chemical and physical methods.

Author Contributions: X.L. performed the experiments and wrote the paper. Z.L., W.H. and H.C. helped with the experiments. X.T., Y.C. (Yeqing Chen) and Y.C. (Yu Chen) provided guidance and

helped in manuscript preparation. All authors have read and agreed to the published version of the manuscript.

Funding: This research was funded by the National Natural Science Foundation (Nos. 51802229 and 12004285), Natural Science Foundation of Guangdong Province (Nos. 2018A030313561 and 2021A1515011935), Guangdong Basis and Applied Fundamental Research Fund (Nos. 2019A1515111190 and 2019A1515110778), Strong School Engineering Fund of Guangdong Province (No. 2020ZDZX2022) and Science Foundation for Young Teachers of Wuyi University (No. 2018td04), Cooperative education platform of Guangdong Province (No. [2016]31), Science and Technology Projects of Jiangmen (Nos. [2017]307 and [2017]149), and Key Laboratory of Optoelectronic materials and Applications in Guangdong Higher Education (No. 2017KSYS011).

Institutional Review Board Statement: Not applicable.

Informed Consent Statement: Not applicable.

Data Availability Statement: Not applicable.

Acknowledgments: The major work was carried out at the School of Applied Physics and Materials and Research Center of Flexible Sensing Materials and Devices in Wuyi University.

Conflicts of Interest: The authors declare no conflict of interest.

References

1. Evعان, D.; Zayim, E. Highly uniform electrochromic tungsten oxide thin films deposited by e-beam evaporation for energy saving systems. *Curr. Appl. Phys.* **2019**, *2*, 198–203. [[CrossRef](#)]
2. Kumar, K.N.; Shaik, H.; Madhavi, V.; Sattar, S.A. On the bonding and electrochemical performance of sputter deposited WO₃ thin films. *IOP Conf. Ser. Mater. Sci. Eng.* **2020**, *872*, 012147. [[CrossRef](#)]
3. Shinde, P.A.; Lokhande, A.C.; Patil, A.M.; Lokhande, C.D. Facile synthesis of self-assembled WO₃ nanorods for high-performance electrochemical capacitor. *J. Alloys Compd.* **2019**, *770*, 1130–1137. [[CrossRef](#)]
4. Zhen, Y.; Jelle, B.P.; Gao, T. Electrochromic properties of WO₃ thin films: The role of film thickness. *Anal. Sci. Adv.* **2020**, *1*, 1–8. [[CrossRef](#)]
5. Leitzke, D.W.; Cholant, C.M.; Landarin, D.M.; Lucio, C.S.; Krüger, L.U.; Gündel, A.; Flores, W.H.; Rodrigues, M.P.; Balboni, R.D.C.; Pawlicka, A.; et al. Electrochemical properties of WO₃ sol-gel thin films on indium tin oxide/poly (ethylene terephthalate) substrate. *Thin Solid Films* **2019**, *683*, 8–15. [[CrossRef](#)]
6. Bouzid, K.; Maindrion, T.; Kanaan, H. Thin-film encapsulated white organic light top-emitting diodes using a WO₃/Ag/WO₃ cathode to enhance light out-coupling. *J. Soc. Inf. Disp.* **2016**, *24*, 563–568. [[CrossRef](#)]
7. Zheng, G.; Wang, J.; Liu, H.; Murugadoss, V.; Zu, G.; Che, H.; Lai, C.; Li, H.; Ding, T.; Gao, Q.; et al. Tungsten oxide nanostructures and nanocomposites for photoelectrochemical water splitting. *Nanoscale* **2019**, *11*, 18968–18994. [[CrossRef](#)] [[PubMed](#)]
8. Shaath, M.; Ansari, M.N.M.; Nordin, N.A.; Al-Furjan, M.S.H. Mechanical properties of tungsten tri-oxide (WO₃) reinforced poly (lactic-acid) (PLA) nanocomposites. *IOP Conf. Ser. Mater. Sci. Eng.* **2021**, *1128*, 012030. [[CrossRef](#)]
9. Bi, Z.; Li, X.; Chen, Y.; Xu, X.; Zhang, S.; Zhu, Q. Bi-functional flexible electrodes based on tungsten trioxide/zinc oxide nanocomposites for electrochromic and energy storage applications. *Electrochim. Acta* **2017**, *227*, 61–68. [[CrossRef](#)]
10. Upadhyay, K.K.; Altomare, M.; Eugénio, S.; Schmuki, P.; Silva, T.M.; Montemor, M.F. On the supercapacitive behaviour of anodic porous WO₃-based negative electrodes. *Electrochim. Acta* **2017**, *232*, 192–201. [[CrossRef](#)]
11. Spanu, D.; Recchia, S.; Schmuki, P.; Altomare, M. Thermal-oxidative growth of substoichiometric WO_{3-x} nanowires at mild conditions. *Phys. Status Solidi RRL* **2020**, *14*, 2000235. [[CrossRef](#)]
12. Mineo, G.; Ruffino, F.; Mirabella, S.; Bruno, E. Investigation of WO₃ electrodeposition leading to nanostructured thin films. *Nanomaterials* **2020**, *10*, 1493. [[CrossRef](#)] [[PubMed](#)]
13. Tu, Y.; Li, Q.; Jiang, D.; Wang, Q.; Feng, T. Microwave intercalation synthesis of WO₃ nanoplates and their NO-sensing properties. *J. Mater. Eng. Perform.* **2015**, *24*, 274–279. [[CrossRef](#)]
14. Cai, G.; Tu, J.; Zhou, D.; Wang, X.; Gu, C. Growth of vertically aligned hierarchical WO₃ nano-architecture arrays on transparent conducting substrates with outstanding electrochromic performance. *Sol. Energy Mater. Sol. Cells* **2014**, *124*, 103. [[CrossRef](#)]
15. Li, Y.; Chen, D.; Caruso, R.A. Enhanced electrochromic performance of WO₃ nanowire networks grown directly on fluorine-doped tin oxide substrates. *J. Mater. Chem. C* **2016**, *4*, 10500–10508. [[CrossRef](#)]
16. Lu, C.H.; Hon, M.H.; Kuan, C.Y.; Leu, I.C. Preparation of WO₃ nanorods by a hydrothermal method for electrochromic device. *Jpn. J. Appl. Phys.* **2014**, *53*, 06JG08. [[CrossRef](#)]
17. Parthibavarman, M.; Karthik, M.; Sathishkumar, P.; Poonguzhali, R. Rapid synthesis of novel Cr-doped WO₃ nanorods: An efficient electrochemical and photocatalytic performance. *J. Iran. Chem. Soc.* **2018**, *15*, 1419–1430. [[CrossRef](#)]
18. Wang, M.; Chen, Y.; Gao, B.; Hao, L. Electrochromic properties of nanostructured WO₃ thin films deposited by glancing-angle magnetron sputtering. *Adv. Electron. Mater.* **2019**, *5*, 1800713. [[CrossRef](#)]

19. Quy, V.H.H.; Jo, I.R.; Kang, S.H.; Ahn, K.S. Amorphous-crystalline dual phase WO₃ synthesized by pulsed-voltage electrodeposition and its application to electrochromic devices. *J. Ind. Eng. Chem.* **2021**, *94*, 264–271. [[CrossRef](#)]
20. Hilliaro, S.; Baldinozzi, G.; Friedrich, D.; Kressman, S.; Strub, K.; Artero, V.; Laberty-Robert, C. Mesoporous thin film WO₃ photoanode for photoelectrochemical water splitting: A sol-gel dip coating approach. *Sustain. Energy Fuels* **2017**, *1*, 145–153. [[CrossRef](#)]
21. Kadam, A.V.; Bhosale, N.Y.; Patil, S.B.; Mali, S.S.; Hong, C.K. Fabrication of an electrochromic device by using WO₃ thin films synthesized using facile single-step hydrothermal process. *Thin Solid Films* **2019**, *673*, 86–93. [[CrossRef](#)]
22. Semenova, A.; Eruzin, A.; Bezrukov, P.; Sychoy, M.; Mjakin, S.; Lukashova, T.; Sudarb, N. Improvement of parameters and conditions for magnetron sputtering of WO₃ layers to enhance their electrochromic performances. *Mater. Today Proc.* **2020**, *30*, 606–610. [[CrossRef](#)]
23. Madhuri, K.V.; Babu, M.B. Studies on Electron Beam Evaporated WO₃ Thin Films. *Mater. Today Proc.* **2016**, *3*, 84–89. [[CrossRef](#)]
24. Tang, X.; Chen, G.; Liao, H.; Li, Z.; Zhang, J.; Luo, J. Unveiling mechanical degradation for a monolithic electrochromic device: Glass/ITO/WO₃/LiClO₄ (PEO)/TiO₂/ITO/glass. *Electrochim. Acta* **2019**, *329*, 135182. [[CrossRef](#)]
25. Brezesinski, T.; Rohlfiing, D.F.; Sallard, S.; Antonietti, M.; Smarsly, B.M. Highly crystalline WO₃ thin films with ordered 3D mesoporosity and improved electro-chromic performance. *Small* **2010**, *2*, 1203–1211. [[CrossRef](#)]
26. Tang, X.; Huang, J.; Liao, H.; Chen, G.; Mo, Z.; Ma, D.; Zhan, R.; Li, Y.; Luo, J. Growth of W₁₈O₄₉/WO_x/W dendritic nanostructures by one-step thermal evaporation and their high-performance photocatalytic activities in methyl orange degradation. *CrystEngComm* **2019**, *21*, 5905–5914. [[CrossRef](#)]
27. Chu, J.; Lan, J.; Lu, D.; Ma, J.; Wang, X.; Wu, B.; Gong, M.; Zhang, R.; Xiong, S. Facile fabrication of WO₃ crystalline nanoplate on FTO glass and their application in electrochromism. *Micro Nano Lett.* **2016**, *11*, 749–752. [[CrossRef](#)]